PAPER • OPEN ACCESS

Structure and superconducting characteristics of magnesium diboride, substitution of boron atoms by oxygen and carbon

To cite this article: Tetiana Prikhna *et al* 2017 *IOP Conf. Ser.: Mater. Sci. Eng.* **279** 012023

View the article online for updates and enhancements.

Structure and superconducting characteristics of magnesium diboride, substitution of boron atoms by oxygen and carbon

Tetiana Prikhna[1], Vitaliy Romaka[2], Michael Eisterer[3], Andrii Shapovalov[1], Artem Kozyrev[1], Gennadiy Grechnev[4], Viktor Boutko[5], Wilfried Goldacker[6], Tobias Habisreuther[7], Oleksii Vakaliuk[8] and Bernd Halbedel[8]

[1]V. Bakul Institute for Superhard Materials of the National Academy of Sciences of Ukraine (NASU), 2, Avtozavodskaya Str., Kiev 07074, Ukraine
[2]Lviv Polytechnic National University, 12 Bandera Str., Lviv, 79013, Ukraine
[3]Atominstitut, TU Wien, Stadionallee 2, 1020 Vienna, Austria
[4]B. Verkin Institute for Low Temperature Physics of the National Academy of Sciences of Ukraine, Kharkov 61103, Ukraine
[5]Donetsk Institute for Physics and Engineering named after O. O. Galkin of the National Academy of Sciences of Ukraine, R. Luxemburg Str. 72, Donetsk-114, 83114, Ukraine
[6]Karlsruhe Institute of Technology (KIT), 76344 Eggenstein-Leopoldshafen, Germany
[7]Leibniz Institute of Photonic Technology e. V., Albert-Einstein-Straße 9, 07745 Jena, Germany
[8]Technische Universität Ilmenau, Institute of Materials Engineering, Gustav-Kirchhoff-Strasse 6, D-98693 Ilmenau, Germany

e-mail of the corresponding author: prikhna@ukr.net

Abstract. An x-ray analysis of MgB_2-based materials shows that they contain MgB_2 and MgO phases. According to a quantitative Auger analysis (taken after removing the oxidized surface layer by Ar ion etching in the microscope chamber) the MgB_2 phase contains some amount of oxygen that approximately corresponds to the composition $MgB_{2.2-1.7}O_{0.4-0.6}$. Rietveld refinement of the MgB_2 phase, based on EDX data with varying B/O content, leads to the composition $MgB_{1.68-1.8}O_{0.2-0.32}$. Ab-initio modelling of boron substitution by oxygen in MgB_2 (ΔH_f =-150.6 meV/atom) shows that this is energetically favourable up to the composition $MgB_{1.75}O_{0.25}$ (ΔH_f =-191.4 meV/atom). In contrast to carbon substitution, where very small levels of doping can dramatically affect the superconducting characteristics of the material with concomitant changes in the electron density, oxygen substitution results in very little change in the superconducting properties of MgB_2. The formation of vacancies at the Mg site of both MgB_2 and substituted $MgB_{1.75}O_{0.25}$ was modelled as well, but has shown that such processes are energetically disadvantageous (ΔH_f of $Mg_{0.875}B_2$ and $Mg_{0.75}B_{1.75}O_{0.25}$ are equal to -45.5 and -93.5 meV/atom, respectively).

1. Introduction

Magnesium diboride has a simple hexagonal structure in which layers of boron atoms alternate with magnesium atom layers [1]. Differently from Y- or Bi-based high temperature superconductors the larger coherence length of MgB_2 makes the superconducting current flow in the material insensitive to the presence of grain boundaries. In fact, grain boundaries and inclusions of secondary phases having sizes commensurable with the coherence length serve as pinning centers for Abrikosov vortices and thus their higher density should correlate with higher critical current densities.

SEM and Auger spectroscopy of the structures of MgB_2-based materials [2-6] prepared by us under different conditions (in flowing Ar, by hot pressing at 30 MPa, by spark plasma sintering at 16-96 MPa, under high quasihydrostatic pressure (2 GPa) – high temperature (600-1100 °C), by high pressure-high temperature treatment of wires, by magnetron sputtering of MgB_2 targets and deposition of thin films) showed that admixed oxygen is present in all materials to a rather high extent [7] due to the high affinity of Mg to oxygen. In bulk superconducting MgB_2 with high critical current densities (see, for example, Fig. 1a) and high critical magnetic fields (Fig. 1d) usually more than two phases are present according to the SEM and Auger data (Fig. 1c): (1) the matrix phase with near MgB_2 stoichiometry which contains a small amount of admixed oxygen; (2) inclusions or grains of higher magnesium borides MgB_x, x>>2 (MgB_4, MgB_7, MgB_{12}, MgB_{17}, MgB_{20}, Mg_2B_{25}, etc.); (3) nanolayers (if the synthesis temperature was low) or separate oxygen enriched inclusions (if it was higher) with near MgBO stoichiometry [7]. The reflections of the higher magnesium borides cannot be detected by x-ray powder diffraction because the inclusions are small, dispersed in the matrix and have big and complicated unit cells. Thus, a lot of small reflections result from the grains of higher borides, which are not seen in the background of the intensive MgB_2 reflections with simple hexagonal structure. The analysis using the FullProf Suite program package for the x-ray patterns revealed the presence of phases with MgB_2 (main phase) and MgO (to a much smaller extent) structures (see, for example Fig. 1a). According to the results of crystal structure refinement, the $2d$ crystallographic site, which should be solely occupied by boron atoms in pure MgB_2, is occupied by a statistical mixture of boron and oxygen in our samples [7]. In all cases the B/O ratio in the $MgB_{2-x}O_x$ solid solution remains practically the same and has nearly the same lattice parameters. No additional reflections that would correspond to the superstructure of $MgB_{2-x}O_x$ were observed. Thus, the analysis using Rietveld refinement allowed us to conclude that the composition of the phase with MgB_2 structure was $MgB_{1.68-1.74}O_{0.26-0.32}$ [7].

A positive effect in enhancing J_c and the upper critical field in MgB_2 materials can be obtained by dopants, in particular by carbon, carbon nanotubes, nanodiamonds or by carbon based additives, e.g. SiC, ethyltoluene, carbohydrates, malic acid, and many others [8-13]. Some carbon goes into the MgB_2 structure and slightly reduces the transition temperature, but the upper critical magnetic field and the irreversibility field increase. If the amount of carbon introduced into MgB_2 is too high, the reduction of the transition temperature annihilates the advantages of its addition.

The present paper also describes the results of *ab initio* calculations of the electronic structure and stability of the MgB_2 compounds with partial oxygen and carbon substitution for boron. The results presented here extend our fist results which were described in [7, 14].

2. Experimental
The microstructure of the materials was characterized by a JAMP−9500F (combined SEM and Auger analyzers) allowing to investigate non-oxidized MgB_2 surfaces (by etching 1×1 mm^2 square surfaces by Ar ions), to perform a quantitative Auger analysis of approximately 10 nm-sized inclusions and to construct depth profiles of the element distribution. The critical current densities, J_c, of the bulks and thin films were estimated from data obtained by an Oxford Instruments vibrating sample magnetometer (VSM) using the Bean model [15]. The values of the upper critical magnetic field, B_{c2}, and the irreversibility field, B_{irr}, were estimated from resistivity measurements (90% and 10% of the resistivity just above the beginning of the transition) using the four probe technique at a current of 10-100 mA and in fields from 0 to 15 T.
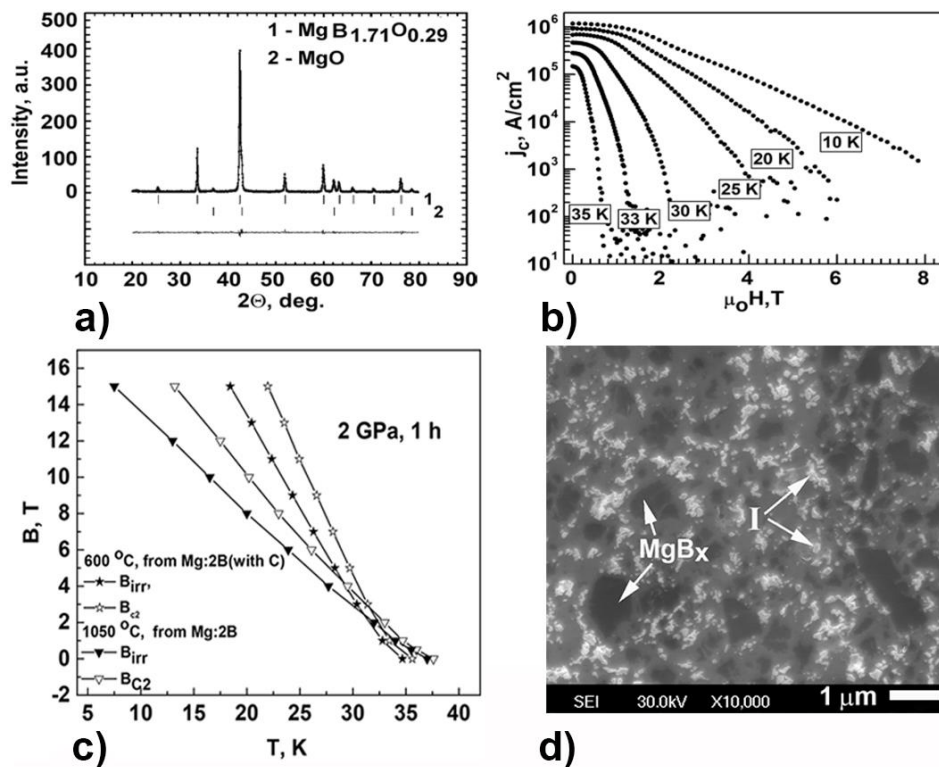
Figure 1. (**a**) - X-ray diffraction pattern, (**b**) – dependence of critical current densities, J_c, on magnetic field, $\mu_o H$, at 10, 20, 25, 30, 33, 35 K and (**d**) - SEM (SEI mode) structure of the material synthesized at 2 GPa, 1050 °C for 1 h from Mg:2B mixture (approximate composition according to the quantitative Auger analysis: matrix – $MgB_{2.2-1.7}O_{0.4-0.6}$, "I" – oxygen enriched inclusions appear brightest - $MgB_{0.6-0.8}O_{0.8-0.9}$; and the boron enriched inclusions "MgB_x" appear darkest – $MgB_{7-13}O_{0.02-0.06}$); (**c**) - dependence of the upper critical magnetic field (B_{c2}) and of the irreversibility field (B_{irr}) of MgB_2-based materials synthesized at 2 GPa for 1h: at 600 °C from Mg:2B (amorphous, contained 3.5 wt% of C) and 1050 °C from Mg:2 B (amorphous, contained 0.47 wt% of C).

The electronic structure of $MgB_{2-x}O_x$ and $MgB_{2-x}C_x$ was obtained using *ab initio* calculations for 2×2×2 and 2×2×1 supercells within the density-functional theory (DFT) [16] by employing the full potential codes: the linearized augmented plane wave method (FP-LAPW with generalized gradient approximation (GGA) [17] implemented in Elk [18] and WIEN2k [19]) and the full-potential LMTO method (FP-LMTO, RSPt implementation [20, 21] with local density approximation (LDA) [22]). All constructed supercells were based on the experimental parameters of the hexagonal MgB_2 cell, a=0.30844 nm and c=0.35215 nm. To analyze the adjusted (refined) positions of atoms and the related binding energies E_b in $MgB_{2-x}O_x$ and $MgB_{2-x}C_x$, WIEN2k [19] was applied.

For the thermodynamic calculation of the enthalpy of formation of binary and ternary compounds, a crystal structure optimization was performed including pure B (116 *k*-points), Mg (84 *k*-points), and the O_2 molecule [18]. The *k*-point mesh size for binary and ternary solids was set to 20×20×10 giving in total 264 (MgB_2) and 462 ($MgB_{1.75}O_{0.25}$) *k*-points in the irreducible part of the unit cell.

X-ray phase analysis was carried out with PowderCell v2.3 [21] using the powder patterns obtained on an X'Pert Pro/PANanalytical diffractometer (Cu K_α radiation, λ = 0.15418 nm) with Bragg-Brentano geometry. Rietveld refinement was performed using the FullProf Suite program package [24].

3. Results and discussion

The discussion in the paper refers to the established by us processing of bulks and wires. Figures 2a, b show isosurfaces of the electron localization function (elf) of MgB_2 (Fig. 2a) and $MgB_{1.75}O_{0.25}$ (Figs. 2b) at elf = 0.7. The strong electron localization in MgB_2 between boron atoms corresponds to strong covalent bonding within the boron network. Substitution of B atom by O leads to electron localization around O atoms and thus bonding polarization (Figs. 2b). Oxygen atoms affect not only the B-O bonds but also nearby B-B bonds by a deformation of the elf. Figure 2c shows the binding energies, E_b, of $MgB_{2-x}O_x/C_x$, i.e. of MgB_2 with oxygen or carbon substitutions at boron positions calculated using WIEN2k. Figure 2d demonstrates the Z - contrast image of coherent oxygen-containing inclusions in MgB_2 [010] bulk material, experimentally obtained by the authors of [26], which confirms that oxygen (when its amount is small) prefers to reside at each second boron plane thus leaving each second boron plane pristine. Figure 3 shows the maps of the electronic density distribution (calculated using WIEN2k) for the pristine MgB_2 structure (Fig. 3a), $MgB_{2-x}O_x$ (Figs. 3b-d) and $MgB_{1.5}C_{0.5}$ (Figs. 3e, f). Figs. 3b-d demonstrate the cases for $MgB_{2-x}O_x$ for x=0.25, (Fig. 3b shows the boron plane with the embedded oxygen atoms in nearby positions, while oxygen atoms are absent in the second boron plane (not shown) of the same unit cell.) and x=0.5. (Fig. 3c shows the boron plane without embedded oxygen atoms, while the second (alternate) boron plane contains these atoms.) Fig.3d displays a selected cut of the unit cell inclined to the basal boron planes to show the boron plane with as well without oxygen and the Mg atoms of the same unit cell. Figure 3e presents the boron plane of the $MgB_{1.5}C_{0.5}$ compound with the position of the embedded carbon atoms resulting in the lowest binding energy. Fig. 2c and Fig. 3f demonstrate selected cuts of the $MgB_{1.5}C_{0.5}$ unit cell to show the boron plane with carbon and the Mg atoms of the same unit cell.

It should be mentioned that for all values of x used for the calculations of the density of states (DOS) near the Fermi level of $MgB_{2-x}O/C_x$ (up to x=1) the densities of state were above zero, i.e. all the compounds show metal-like behaviour. In the case of $MgB_{2-x}O_x$ the lowest DOS (about 0.46 states/eV/f.u.) was found for $MgB_{1.75}O_{0.25}$ if the oxygen atoms are in neighbouring positions [7]. If the concentration of oxygen is higher than in $MgB_{1.5}O_{0.5}$ the MgB_2 structure is destroyed. In the case of $MgB_{2-x}C_x$ the lowest DOS (about 0.3 states/eV/f.u.) was found for $MgB_{1.5}C_{0.5}$, when carbon distributed homogeneously (i.e. is introduced in both basal boron planes of the same 2×2×2 MgB_2 supercell [25]). The maps of the electron density distribution were calculated under the assumption that the oxygen or carbon atoms substituting boron can be shifted from the positions occupied by boron because of the size difference of the atomic radii and the amount of electrons in their atoms.

The binding energy was calculated under the assumption of a homogeneous (curves 1 and 3) distribution of oxygen or boron in the MgB_2 structure and, in parallel, for the case of a so-called ordered distribution of the substituted atoms. This means that we calculated maps for substitutions where oxygen atoms occupy nearby or alternative boron positions and when they move into one or two boron planes of the unit cell.

The curves 2 and 4 (Fig. 2c) correspond to the lowest E_b for each concentration of oxygen atoms (distributed in definite order or randomly). The lowest E_b is observed when oxygen moves into nearby positions or form zigzag chains (curve 2, Fig. 2c), while in the case of carbon there was no difference (curves 3 and 4, Fig. 2c). Therefore, the lower E_b in the case when oxygen moves into nearby positions can explain the tendency of its segregation in the MgB_2 structure and the formation of oxygen-enriched inclusions as well as why a rather high amount of oxygen can be present in superconducting MgB_2 with a high transition temperature.

The imbedding of carbon into the MgB_2 structure is preferable in any case. It does not make any difference whether it substitutes boron in a special order or homogeneously, i.e. introducing carbon into both boron planes of the unit cell. Thus, if the concentration of carbon atoms is high, the transition temperature and superconductivity of MgB_2 are essentially suppressed. Fig. 1c shows the upper critical magnetic fields and the irreversibility fields of MgB_2-based material prepared from boron to which carbon was specially added (3.5 wt%). Usually 0.31-0.47 wt% of carbon are present in amorphous boron. Despite the very high critical magnetic fields, the T_c of the material is reduced to 34 K and not
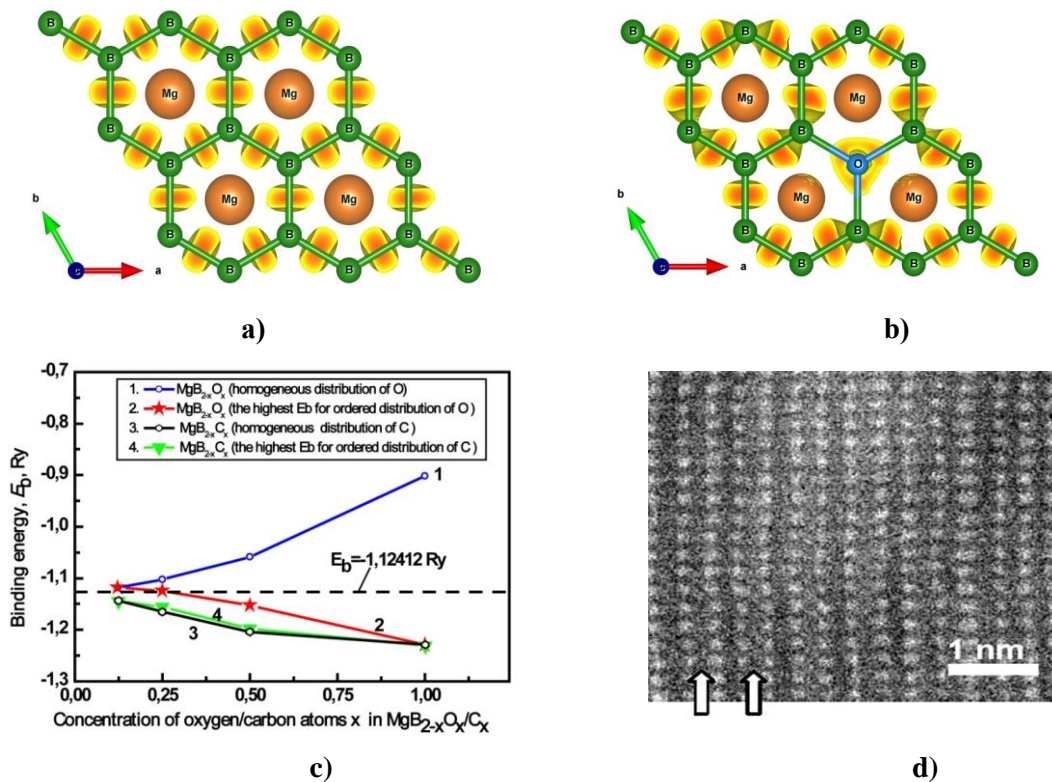
Figure 2. (a, b) - Isosurfaces of the electron localization function (elf) of MgB_2 and $MgB_{1.75}O_{0.25}$ at elf = 0.7; (c) - Dependence of the binding energy, E_b, on the oxygen concentration, x, in $MgB_{2-x}O_x/C_x$: 1, 3- homogeneous oxygen and carbon substitutions for boron atoms, respectively; 2, 4 - the lowest binding energy for each x in the case of ordered oxygen and carbon substitutions (for example, in the nearby positions or in pairs), respectively; (d) - Z - contrast image of coherent oxygen-containing inclusions in MgB_2 [010] bulk [26]. Bright atoms - Mg. The contrast increases in each second row and is due to the presence of oxygen in each second boron plane. The white arrows show the columns of atoms in which oxygen is present.

Table 1. Calculated enthalpies of formation of MgB_2, MgO, $Mg_{1-x}B_2$, and $MgB_{2-x}O_x$

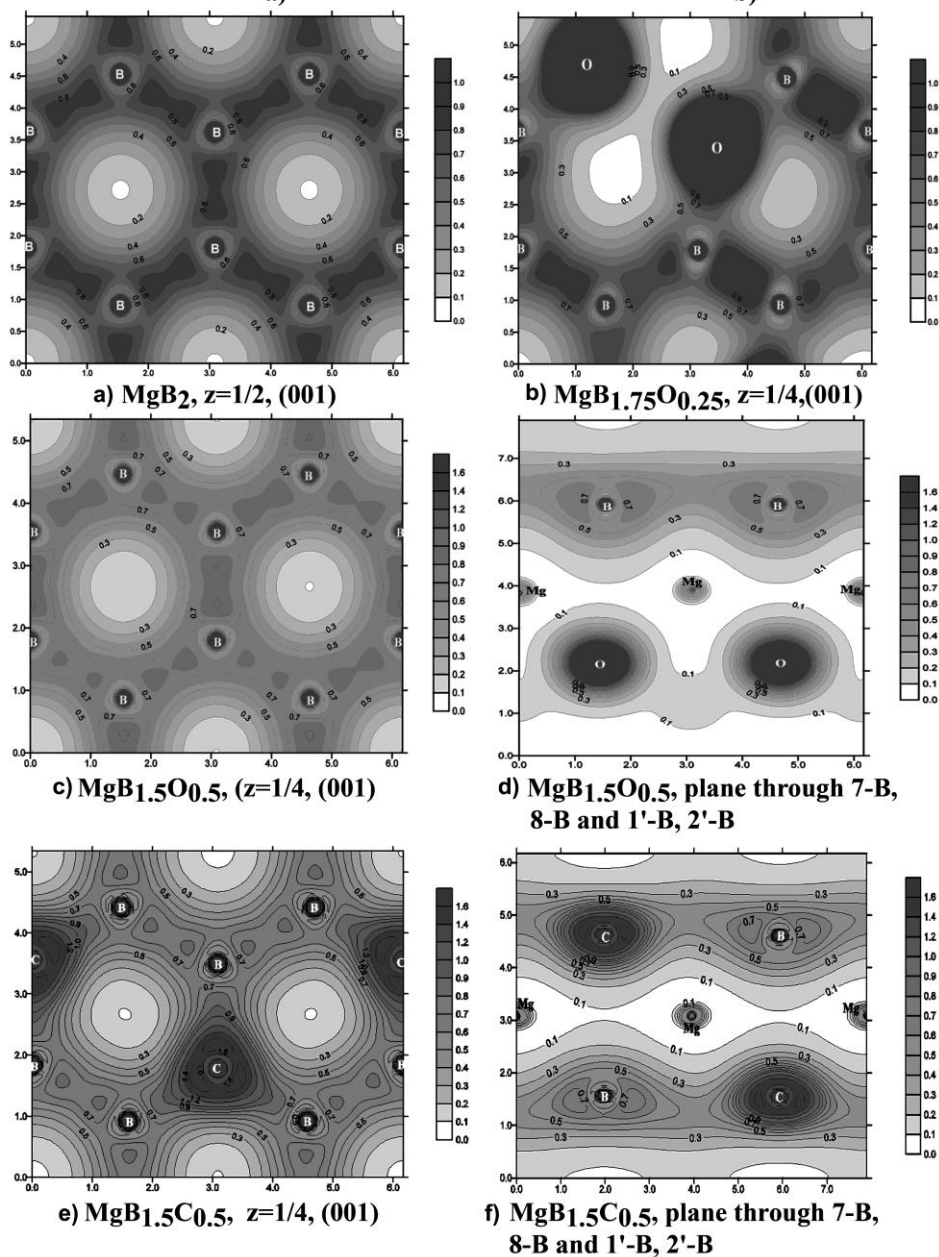| No	Compound	Enthalpy of formation, ΔH_f (meV/atom)
1	MgB_2	-150.6
2	$Mg_{0.875}B_2$	-45.5
3	$Mg_{0.75}B_2$	+74.6
4	$Mg_{0.75}B_{1.75}O_{0.25}$	-93.5
5	$MgB_{1.75}O_{0.25}$	-191.4
6	$MgB_{1.5}O_{0.5}$	-162.6
7	MgO	-2719.7
8	$MgO_{0.5}B_{0.5}$	-82.0

Figure 3. Maps of electron density distribution for: (a) - MgB_2 (z=1/2, (001)), (b) - $MgB_{1.75}O_{0.25}$ (z=1/4,(001) [7]), (c) - $MgB_{1.5}O_{0.5}$ (z=1/4, (001)); z- coordinates of the plane of a 2×2×2 supercell, where z is given in units of the *c* parameter of a 2×2×2 MgB_2 supercell [25]; (d) – $MgB_{1.5}O_{0.5}$ in the transversal plane under an angle to the basal boron planes of the hexagonal unit cell, in order to show the boron plane without imbedded oxygen atoms together with the Mg plane (i.e., the plane which goes through 7-B, 8- B and 1'-B, 2'-B positions of a 2×2×2 supercell [25]); (e) - $MgB_{1.5}C_{0.5}$ (z=1/4, (001)); (f) - $MgB_{1.5}C_{0.5}$ in the transversal plane under an angle to the basal boron planes (the plane which goes through 7-B, 8- B and 1'-B, 2'-B positions of a 2×2×2 supercell).

all carbon added to boron is imbedded into the MgB_2 structure, only about 0.050 at%, while according to our estimations the amount of imbedded carbon was around 0.0028 at% in materials with T_c near

38 K. However, these values are obtained from the lattice parameter which is likely influenced by the simultaneous oxygen substitution as well.

Table 1 shows the results of our calculations of the formation enthalpy, ΔH_f, for MgB_2, MgO, $Mg_{1-x}B_2$, and $MgB_{2-x}O_x$. The calculations of MgB_2 structures with a deficit of Mg were performed because this could as well be the reason for the deviation of composition from stoichiometric MgB_2. But, as the results presented in the Table 1 show, this is energetically disadvantageous. Moreover, the formation of vacancies in the Mg crystallographic site with simultaneous substitution of B by O is still less favorable than the formation of pure MgB_2 or even $MgB_{2-x}O_x$.

The formation enthalpy of MgO is very high (exothermal process) and the introduction of boron into the MgO structure dramatically decreases $-\Delta H_f$. The formation of $MgB_{0.6-0.8}O_{0.8-0.9}$ inclusions found in our experiments remains so far unclear. Further calculations are in progress for a clarification. However, phases which are unexpected from enthalpy considerations of the isolated compound may form in a multicomponent system, such as TiH_2 in titanium doped MgB_2 [27].

4. Conclusions

Ab initio calculations of the DOS, of maps of the electron density distribution and of the formation enthalpy of $MgB_{2-x}O_x/C_x$ structures have been performed. The results show that it is most favourable in the case of oxygen substitution for boron to form the $MgB_{1.75}O_{0.25}$ compound (if oxygen substitutes boron in nearby positions). Very similar compositions were observed experimentally in MgB_2-based materials with very good superconducting characteristics. Further modelling is necessary to clarify the formation of nanolayers and inclusions with near MgBO stoichiometry, which were observed experimentally in MgB_2-based materials.

5. References

[1]   C. Buzea and T. Yamashita, Review of superconducting properties of MgB_2, *Supercond. Sci. Technol.* 14(11), R115 (2001) doi:10.1088/0953-2048/14/11/201.
[2]   T. Prikhna, M. Eisterer, H.W. Weber, W. Gawalek, V. Kovylaev, M. Karpets, V. Moshchil, A. Kozyrev, T. Basyuk, X. Chaud, W. Goldacker, V. Sokolovsky, J. Noudem, A. Borimskiy, V. Sverdun, E. Prisyazhnaya, Temperature-pressure induced nano-structural inhomogenities for vortex pinning in bulk MgB_2 of different connectivity, *Physica C* 503, 109-112 (2014).
[3]   T.A. Prikhna, M. Eisterer, H.W. Weber, W. Gawalek, V.V. Kovylaev, M.V. Karpets, T.V. Basyuk and V.E. Moshchil, Nanostructural inhomogeneities acting as pinning centers in bulk MgB_2 with low and enhanced grain connectivity, *Supercond. Sci. Technol.* 27(4), 044013 (9pp) (2014).
[4]   T. Prikhna, M. Eisterer, W. Gawalek, A. Kozyrev, H.W. Weber, V. Sokolovsky, X. Chaud, J. Noudem, T. Habisreuther, V. Moshchil, M. Karpets, T. Basyuk, V. Kovylaev, J. Dellith, V. Sverdun, R. Kuznietsov, C. Shmidt, T. Vitovetskaya, L. Polikarpova, Synthesis Pressure–Temperature Effect on Pinning in MgB_2-Based Superconductors, *J. Supercond. Nov. Magn.* 26, 1569–1576 (2013).
[5]   T. Prikhna, W. Gawalek, M. Eisterer, H. Weber, M. Monastyrov, V. Sokolovsky, J. Noudem, V. Moshchil, M. Karpets, V. Kovylaev, A. Borimskiy, V. Tkach, A. Kozyrev, R. Kuznietsov, J. Dellith, C. Shmidt, D. Litzkendorf, F. Karau, U. Dittrich, M. Tomsic, The effect of high-pressure synthesis on flux pinning in MgB_2-based superconductors, *Physica C: Superconductivity.* 479, 111-114 (2012).
[6]   T. Prikhna in: *Structure and properties of bulk MgB_2 // Superconducting Wires: Basics and Applications,* edited by R. Fluekiger, World Scientific Series in Applications of Superconductivity and Related Phenomena., p. 131-157 (668 pp.) (2016).
[7]   T.A. Prikhna, V.V. Romaka, A.P. Shapovalov, M. Eisterer, V. Sokolovsky, H.W. Weber, G.E. Grechnev, V.G. Boutko, A.A. Gusev, A.V. Kozyrev, W. Goldacker, V.E. Moshchil, V.B. Sverdun, T. Habisreuther, C. Schmidt, V.V. Kovylaev, V.E. Shaternik, M.V. Karpets, A.V. Shaternik, Structure and Properties of MgB_2 Bulks, Thin Films, and Wires, *IEEE Transactions*

on Applied Superconductivity, 27(4),   1 (2017) DOI: 10.1109/TASC.2016.2638201

[8]   E.W. Collings, M.D. Sumption, M. Bhatia, M.A. Susner and S.D. Bohnenstiehl, Prospects for improving the intrinsic and extrinsic properties of magnesium diboride superconducting strands, *Supercond. Sci. Technol.* 21(10) 103001 (2008).

[9]   S.X. Dou, O. Shcherbakova, W.K. Yeoh, J.H. Kim, S. Soltanian, X.L. Wang, C. Senatore, R. Flukiger, M. Dhalle, O. Husnjak and E. Babic, Mechanism of Enhancement in Electromagnetic Properties of MgB_2 by nano SiC doping, *Phys. Rev. Lett.,* 98, 097002 (2007) doi: 10.1103/PhysRevLett.98.097002.

[10]   J.H. Kim, S. Oh, Y-Uk Heo, S. Hata, H. Kumakura, A. Matsumoto, M. Mitsuhara, S. Choi, Y. Shimada, M. Maeda, J.L. MacManus-Driscoll, S.X. Dou, Microscopic role of carbon on MgB_2 wire for critical current density comparable to NbTi, *NPG Asia Materials* 4, e3 (2012); doi:10.1038/am.2012.3.

[11]   X.L. Wang, S. Soltanian, M. James, M.J. Qin, J. Horvat, Q.W. Yao, H.K. Liu and S.X. Dou, Significant enhancement of critical current density and flux pinning in MgB_2 with nano-SiC, Si, and C doping, *Physica C* 408-410, 63-67 (2004).

[12]   Y.B. Zhang, X.J. Shan, X.W. Bai, T.Y. Liu, H.M. Zhu and Ch.B. Cai, In situ synthesis and current-carrying characteristics of superconducting MgB_2–B_4C composites with MgB_2 fractions ranging from 18% to 85%, *Supercond. Sci.Technol.,* 25, 095003 (2012).

[13]   H. Yamada, N. Uchiyama, A. Matsumoto, H. Kitaguchi and H. Kumakura, The excellent superconducting properties of *in situ* powder-in-tube processed MgB_2 tapes with both ethyltoluene and SiC powder added, *Supercond. Sci. Technol.* 20, L30 (2007).

[14]   T. Prikhna, A. Shapovalov, M. Eisterer, V. Shaternik, W. Goldacker, H.W. Weber, V. Moshchil, A. Kozyrev, V. Sverdun, V. Boutko, G. Grechnev, A. Gusev, V. Kovylaev, A. Shaternik, Pinning in high performance MgB_2 thin films and bulks: Role of Mg-B-O nano-scale inhomogeneities, *Physica C: Superconductivity and its applications* 533, 36–39 (2017).

[15]   Bean, C. B., Magnetization of high field superconductors, *Rev. Mod. Phys.* 36, 31-36 (1964).

[16]   R.G. Parr and W. Yang, Density-Functional Theory of Atoms and Molecules, Oxford Univ. Press, (1989), e-book.

[17]   J.P. Perdew, S. Burke, and M. Ernzerhof, Phys. Rev. Lett. 77, 3865 **(**1996).

[18]   ELK, Program package; http://elk.sourceforge.net/.

[19]   P. Blaha, K. Schwarz, G.K.H. Madsen *et al.,* WIEN2K, An augmented plane wave + local orbitals program for calculating crystal properties, Techn. Univ., Wien (2001).

[20]   J.M. Wills, M. Alouani, P. Andersson, A. Delin, O. Eriksson, and A. Grechnev, Full-Potential Electronic Structure Method. Energy and Force Calculations with Density Functional and Dynamical Mean Field Theory, Berlin: Springer, (2010) e-book.

[21]   http://fplmto-rspt.org/

[22]   U. von Barth, L. Hedin, A local exchange-correlation potential for the spin polarized case I, *J. Phys. C: Solid State Phys*. 5, 1629, (1972).

[23]   W. Kraus, G. Nolze, Powder Cell for Windows. – Berlin (1999).

[24]   Rodríguez-Carvajal, J. Recent Developments of the Program FULLPROF, in Commission on Powder Diffraction (IUCr). Newsletter, 26, 12-19 (2001)

[25]   T.A. Prikhna, A.P. Shapovalov, G.E. Grechnev, V.G. Boutko, A.A. Gusev, A.V. Kozyrev, M.A. Belogolovskiy, V.E. Moshchil and V.B. Sverdun, Formation of nanostructure of magnesium diboride based materials with high superconducting characteristics, *Low Temperature Physics* 42(5), 486–505 (2016).

[26]   R.F. Klie, J.C. Idrobo, N.D. Browning, A. Serquis,Y.T. Zhu, X.Z. Liao, and F.M. Mueller, Observation of coherent oxide precipitates in polycrystalline MgB_2, *Appl. Phys. Lett.* 80, 3970-3972 (2002).

[27]   S. Haigh, P. Kovac, T. A. Prikhna, Ya.M. Savchuk, M. Kilburn, C. Salter, J. Hutchison, C. Grovenor, Chemical interactions in Ti doped MgB_2 superconducting bulk samples and wires *Supercond. Sci. Technol.* 18, 1–7 (2005) doi:10.1088/0953-2048/18/0/000